Fluorocarbons Dissolved in Supercritical Carbon Dioxide. NMR Evidence for Specific Solute−Solvent Interactions

Alexander Dardin,† Joseph M. DeSimone, and Edward T. Samulski*

CB#3290 Venable and Kenan Laboratories, Department of Chemistry, University of North Carolina at Chapel Hill, Chapel Hill, North Carolina 27599-3290

Received: July 1, 1997; In Final Form: October 27, 1997

The proton and fluorine chemical shifts of *n*-hexane, perfluoro-*n*-hexane, and 1,1-dihydroperfluorooctylpropionate dissolved in supercritical carbon dioxide have been studied using high-pressure, high-resolution nuclear magnetic resonance. The CO_2 density differentially influences ^1H and ^{19}F chemical shifts, which, in turn, suggest specific solute−solvent interactions between CO_2 and fluorinated compounds. The density-dependent proton chemical shifts are exclusively governed by changes in the bulk susceptibility of CO_2; these shifts exhibit only a slight temperature dependence. By contrast, the ^{19}F signals show that an additional mechanism—a van der Waals term—contributes to the magnetic shielding, and this has to be taken into account to explain the experimental shifts as a function of CO_2 density and temperature. Furthermore, the ^{19}F NMR data also show a distinct site specificity which is qualitatively explained in terms of the surface accessibility of fluorine atoms in the various $CF_2(CF_3)$ units in fluorocarbons.

Introduction

We use NMR to probe specific interactions between CO_2 and fluorinated molecules in fluid phases of CO_2. Liquid and supercritical CO_2 are receiving growing scientific and industrial attention because of CO_2's unique solvent properties.[1−4] For example, its density, viscosity, dielectric constant, and solubility parameter can be varied over a wide range from gaslike phases to liquidlike ones. CO_2 dissolves many different low molar mass compounds[5−7] and can also plasticize various polymers.[8,9] Additionally, liquid and supercritical CO_2 can act as a substitute solvent for the environmentally harmful chlorofluorocarbons (CFCs) in the synthesis of certain fluoropolymers.[4,10] Since polymer solubility is restricted to two particular classes of polymeric systems—amorphous fluorinated polymers and silicone polymers—there is interest in surface-active, amphiphilic macromolecules. Surfactants are essential for exploiting CO_2 as a solvent for heterogeneous reactions.[11] Recent examples of such macromolecular amphiphiles are composed of "CO_2-philic" and "CO_2-phobic" segments, and these surfactants stabilize CO_2-insoluble species including polymeric compounds in CO_2.[11−13]

To design surfactants with tailored solubility in CO_2, knowledge of the intermolecular amphiphile−solvent interactions is essential. To date, however, little is known about the origin of the solvation power of CO_2, in particular the origin of the exceptional solubility of fluorinated polymeric compounds. CO_2 has a modest polarizability, no dipole moment, and a large quadrupole moment. On the other hand, relative to hydrogenated molecules, fluorinated compounds differ dramatically in size, electronegativity and polarity. Various theoretical approaches including ab initio calculations have been applied to this problem. CO_2 solubility is correlated with the ability of a solute to participate in electrostatic interactions[14] or the acidity/basicity of CO_2 (in analogy to Pearson's model of soft and hard acids and bases[15]). The latter model was applied by Meredith et al. to determine equilibrium constants of systems containing CO_2 and different Lewis bases.[16] Yee et al.[17] anticipated increased interactions between the quadrupole moment of CO_2 and the dipoles of CF_2 and CF_3 units. In their IR spectroscopic investigations, however, they did not observe any evidence for specific interactions. Recent calculations of Cece and coworkers indicated increased interactions between CO_2 and a fluorocarbon in comparison to the corresponding hydrocarbon.[18] The high-pressure NMR investigations presented here support these findings and give some insights into solute−solvent interactions in supercritical CO_2.

Background

Various spectroscopic methods such as UV absorbance, fluorescence emission, IR, electron spin resonance, and nuclear magnetic resonance spectroscopy have been applied to examine solubility, solute−solvent interactions, and the formation of complexes in supercritical solutions.[19,20] Since the work of Dickinson[21] 45 years ago, high-resolution NMR spectroscopy has played an important role in the study of medium effects and their molecular origins.[22,23] The bulk medium surrounding a solute contributes to the magnetic field at the solute nuclei, H_{eff}, in a way that depends on the sample geometry. In the case of a cylindrical sample parallel to the external magnetic field, H_{eff} is given by

$$H_{eff} = (1 - \sigma)H_0 = H_0[1 + (4\pi/3)\chi_v] \qquad (1)$$

where H_0 is the external magnetic field strength and χ_v is the diamagnetic volume susceptibility of the medium. This defines the shielding, σ_b, due to the bulk susceptibility of the medium:

$$\sigma_b = -\frac{4\pi}{3}\chi_v = -\frac{4\pi\chi_m}{3V_m} = -\frac{4\pi\chi_m}{3M}\rho \qquad (2)$$

χ_m refers to the molar susceptibility, V_m is the molar volume,

* To whom correspondence should be addressed.
† Current address: RohMax Additives, 64293 Darmstadt.

S1089-5647(97)02127-5 CCC: $15.00
Published on Web 02/12/1998

M is the molecular weight, and ρ is the density of the medium. In the first systematic investigations of medium effects by NMR, Bothner-By and Glick[24] correlated the density of the medium with the bulk susceptibility according to eq 2. The observed "excess shifts" were subsequently attributed to van der Waals forces[25] giving rise to a shielding term, σ_w, which contributes to the shift in addition to the contribution from σ_b. A variety of continuum and pair interaction models have been developed to obtain a quantitative understanding of σ_w. (For a detailed review see Chapters 2 and 3 in ref 22 and the references therein.) In all of the models, the important parameters are the polarizabilities, $\alpha_{1,2}$, the ionization potentials, $I_{1,2}$, and the molar volumes, $V_{1,2}$, of the solute (index 1) and the solvent (index 2). Further improvements in modeling considered a site factor (due to a different accessibility of individual positions in a solute molecule[26,27]), a coordination number, (i.e., the number of nearest-neighboring solvent molecules[28]), and a quantum mechanical description of interacting atoms.[29] In these models, the knowledge of the chemical shift of the isolated molecule σ_0—which had to be determined from NMR experiments in the gas phase—was necessary. However, most studies were performed on rather simple model substances of which all of the above-mentioned parameters were known, and often different reference standards were used, complicating the results for the absolute contribution of σ_w.

In our studies, which include a comparison of ^{1}H and ^{19}F chemical shifts as a function of solvent parameters (density, temperature), we investigated the relative contribution of σ_w to the chemical shift of a solute in supercritical CO_2. Therefore, we are not able to make statements about the absolute magnitude of the van der Waals contributions to the chemical shift. However, we can follow such intermolecular interactions as a function of CO_2 pressure and temperature.

Experimental Section

n-Hexane (*n*-C_6H_{14}) and perfluoro-*n*-hexane (*n*-C_6F_{14}) were purchased from Aldrich and used without further purification. 1,1-Dihydroperfluorooctylpropionate (FOP) has been prepared from 1,1-dihydroperfluorooctylacrylate (FOA, obtained from 3M) by standard heterogeneous hydrogenation methods using a Wilkinson catalyst.[30]

High-Pressure ^{1}H NMR Experiments. High-resolution ^{1}H and ^{19}F NMR spectra were recorded on a Bruker MSL-360 spectrometer operating at a proton frequency of 360.13 MHz (8.455 T) and a fluorine frequency of 338.38 MHz, respectively. The length of the 90° pulse was 4.95 μs for protons and 5.1 μs for fluorine. For the ^{19}F NMR experiments an echo pulse sequence (Hahn echo) was applied to avoid baseline distortion due to probe ringing. A recycle delay of 5 s ($>5T_1$) was used for all experiments.

The high-pressure setup utilized herein was based on the cell design of Yonker et al.[31,32] which was interfaced with our standard high-pressure equipment. The high-pressure NMR cell consists of a polyimide-coated glass capillary (Polymicro Tech.) with an inner diameter of 150 μm. The capillary was folded repeatedly (21 times with a fold length of 5 cm) and fits into a regular 5 mm NMR tube, which in turn was attached to a 70 cm glass tube conduit for the capillary out of the top opening of the magnet. One end of the capillary was connected to a custom-made, 2.5 mL stainless steel high-pressure view cell interfaced with a pressure generator pump using standard high-pressure valves and tubing (High Pressure Equipment, HIP) the other end was sealed with a high-pressure valve. The total volume of this setup including view cell, valves, and tubing is 6.4 mL.

The space surrounding the folded capillary in the NMR tube was filled with $CDCl_3$ which was used as an external lock solvent. The temperature in the observation region of the capillary was controlled by the Bruker VT-1000 unit which was calibrated against an external thermocouple and was constant within ±1 K. Pressure up to 350 bar was applied by a hand-driven pressure generator (HIP) and measured with a calibrated pressure transducer (Sensotec).

Prior to recording the NMR spectra, 50 mg of the sample substance was first placed in the high-pressure view cell and pressurized with CO_2 (Air Products) to 300 bar to give a 2 wt/vol % solution. The mixture was stirred with a magnetic stir bar, and a homogeneous solution was obtained. After connecting the external setup to the capillary, the CO_2 solution was allowed to flow into the capillary. Air initially in the capillary was flushed out by opening the valve at the end of the capillary. (The volume of the capillary tubing is essentially negligible relative to the volume of the high-pressure setup, resulting in only a short and small pressure drop during this process.) The pressure of the system and the temperature in the NMR probe were set to the desired value and determined to be stable over a period of 1 h.

Pressure-dependent NMR Experiments were carried out starting at low CO_2 densities, i.e., a pressure of about 100 bar at temperatures of 41.2, 52.9, and 64.6 °C. After each incremental pressure change (of about 10−25 bar), the system was allowed to equilibrate until the pressure reading was stable for at least 20 min. The pressure in the system was then constant within ± 0.345 bar (±5 psi on the instrument).

The proton chemical shifts were referenced with respect to the residual protons in the $CDCl_3$ surrounding the capillary; ^{19}F chemical shifts were measured relative to $CFCl_3$ (5% in $CDCl_3$).

Results and Discussion

***n*-C_6H_{14} in Supercritical CO_2.** Proton NMR spectra of *n*-hexane in supercritical CO_2 were recorded with increasing CO_2 pressures from 85.9 to 341.2 bar at constant temperatures of 41.2 and 64.6 °C, respectively. The corresponding densities were calculated according to the method of Ely[33] and ranged from 0.21 g cm^{-3} (4.72 mol L^{-1}) to 0.93 g cm^{-3} (21.04 mol L^{-1}). No corrections due to the amount of the dissolved solute were applied. Figure 1 shows the ^{1}H chemical shifts of *n*-hexane in supercritical CO_2 as a function of CO_2 density. For both of the resonances, CH_3 and CH_2, there is a linear relationship between chemical shift and the density of CO_2 with slopes of -1.84×10^{-6} and -1.87×10^{-6} cm^3 g^{-1}, respectively. For the solute protons in carbon dioxide, the proportionality factor between the magnetic shielding σ_b and the density of the solvent can be calculated from eq 2. Using the volume magnetic susceptibility of CO_2 given in the literature[34] ($\chi_v = 0.473 \times 10^{-6}$), the expected slope is -1.98×10^{-6} cm^3 g^{-1}, about 7% and 5.6% higher than the slope experimentally obtained from the methyl and methylene protons, respectively. We attribute these small deviations to the neglect of the effect of the solute on density and susceptibility and to the less than ideal parallel alignment of the folded capillary in the NMR coil.

Although we cannot rule out the possibility of a constant contribution from σ_w to the observed proton chemical shift, our experiments clearly show that there are no density-dependent factors contributing to the proton shielding other than the bulk susceptibility of CO_2. Second, as expected, this contribution to the shielding is identical for all of the protons in *n*-hexane independent of their position along the hydrocarbon chain; i.e., there is no site-specific interaction. These findings are in general

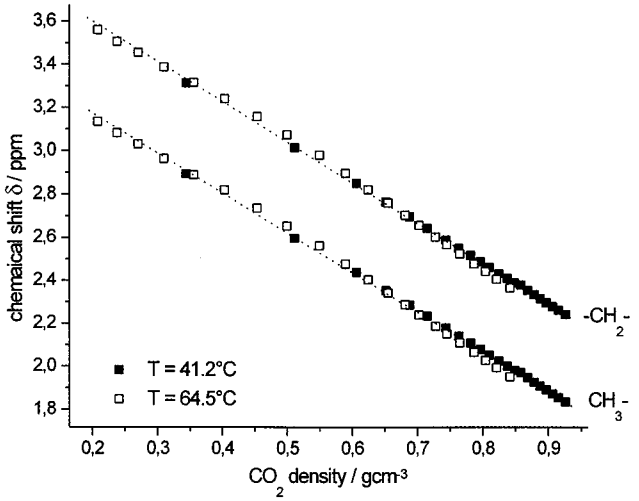

Figure 1. ^{1}H chemical shifts of *n*-hexane at $T = 41.2$ °C (filled symbols) and $T = 64.6$ °C (open symbols) versus CO_2 density. The circles refer to the CH_3 resonances and the squares to the maximum of the CH_2 multiplet. The spectra were recorded with 256 transients. Chemical shifts are measured with respect to $CDCl_3$.

agreement with published data for the van der Waals contribution to chemical shifts of nonpolar solutes in a nonpolar solvent; they are found to be very small ($\sigma_w \leq 0.2$ ppm). The calculations by Cece et al.[19] also suggested that there are no, or only minor, interactions between hydrocarbons and CO_2. Finally, increasing the temperature to 64.6 °C results only in small deviations from the data observed at 41.2 °C, mainly at higher CO_2 densities. Since the molar bulk susceptibility χ_m can be assumed to be temperature independent,[35] we see no evidence for any distinct temperature effect on the proton chemical shift of *n*-hexane in supercritical CO_2.

***n*-C_6F_{14} in Supercritical CO_2.** We next consider the ^{19}F NMR data of perfluoro-*n*-hexane (*n*-C_6F_{14}) in CO_2. Again, the chemical shifts were measured as a function of CO_2 density in a range from 0.23 to 0.93 g cm^{-3} at three different temperatures (41.2, 52.9, and 64.6 °C). The data are displayed in Figure 2.

It is obvious that the behavior of the ^{19}F chemical shift of perfluoro-*n*-hexane with changing CO_2 density is entirely different from that of its hydrogenated analogue (contrast Figure 1 and Figure 2). Four main observations can be discussed from these experiments:

(1) Most importantly, with increasing CO_2 density the chemical shifts do not follow the trend of the bulk susceptibility which, according to eq 2, would result in a continuous upfield shift (of about −1.4 ppm over the observed density range). Instead, depending on the temperature, small upfield shifts (about −0.1 ppm for the β-CF_2 units) but also downfield shifts of up to 0.4 ppm (CF_3 unit at $T = 64.6$ °C) are visible. Consequently, the bulk susceptibility is not the only contribution to the magnetic shielding of the ^{19}F nuclei in CO_2. The additional contributions can be understood as follows: In general, the observed chemical shift, σ, can be written in terms of a virial expansion[37]

$$\sigma = \sigma_0 + \frac{\sigma_1}{V_m} + \frac{\sigma_2}{V_m^2} + ... \qquad (3)$$

where σ is the shielding in a medium, σ_0 is the shielding of the solute in vacuo, and V_m is the molar volume of the medium. Following the pair interaction model by Raynes et al.,[38] σ_1 refers to the second virial coefficient of the shielding (corresponding to binary collisions) and can be split into factors due to bulk

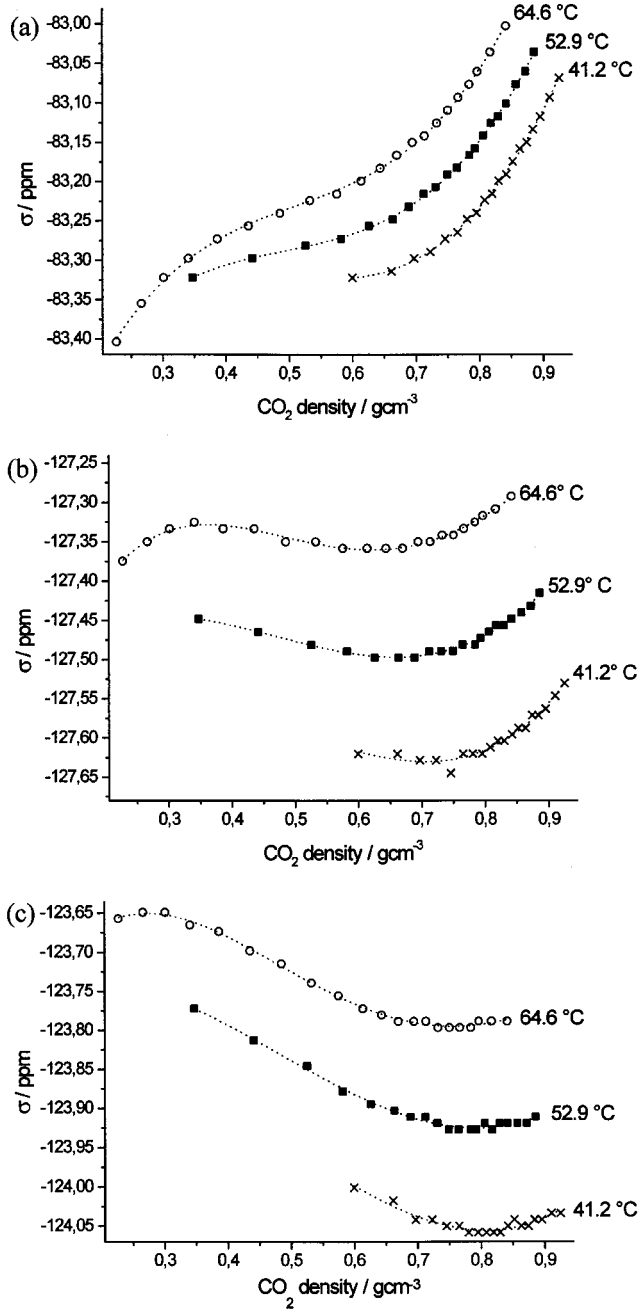

Figure 2. ^{19}F chemical shifts of the perfluoro-*n*-hexane units in CO_2 as a function of the CO_2 density and temperature: (a) CF_3, (b) α-CF_2, and (c) β-CF_2. Spectra were taken with 256 scans, and peak assignments are based on ^{19}F−^{19}F COSY experiments of perfluoro-n-hexane in $CDCl_3$.[36]

susceptibility (σ_b), van der Waals forces (σ_w), dipole−dipole interactions (σ_E), and anisotropy effects (σ_a):

$$\sigma_1 = \sigma_b + \sigma_w + \sigma_E + \sigma_a \qquad (4)$$

For the nonpolar carbon dioxide, dipole−dipole interactions can be excluded, and the term due to the anisotropy of the molecules is in general very small. Thus, the additional shielding observed in the ^{19}F NMR experiments would appear to be due to intermolecular van der Waals forces between the perfluoro-*n*-hexane solute and the CO_2 solvent molecules.

(2) It is striking that none of the curves in Figure 2 are a linear function of solvent density. While for the fit of the data points at 41.2 °C a second-order polynomial is sufficient, third-

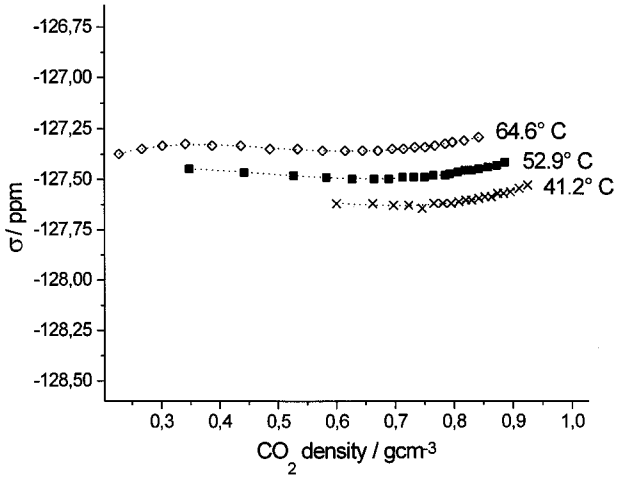

Figure 3. ^{19}F chemical shifts of the α-CF_2 unit in perfluoro-*n*-hexane in CO_2 versus density measured at three different temperatures. The value of the chemical shifts are given with respect to $CFCl_3$ (5% in $CDCl_3$).

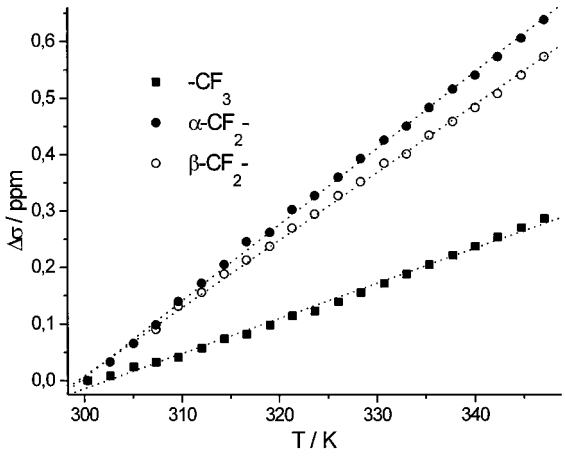

Figure 4. Changes in the fluorine chemical shifts of perfluoro-*n*-hexane dissolved in supercritical CO_2. The spectra were taken at a constant density of 0.68 g cm^{-3} while the temperature was varied. For better comparison a presentation of the absolute change of the chemical shift is chosen ($\Delta\sigma = \sigma - \sigma_{initial}$).

and fourth-order polynomials are necessary to reproduce the observed trends of the chemical shifts at higher temperatures. A nonlinear behavior of chemical shift curves as a function of pressure or density has also been reported in the literature.[39,40] In terms of the Raynes model[38] eq 3 can also be rewritten as a function of density at constant temperature:

$$\sigma(T,\rho) = \sigma_0(T) + \sigma_1(T)\left(\frac{\rho}{M}\right) + \sigma_2(T)\left(\frac{\rho}{M}\right)^2 + \ldots \qquad (5)$$

Therein, terms of third and higher order have to be attributed to ternary and higher order interactions between solute and solvent molecules.

(3) Perfluoro-*n*-hexane exhibits three chemically inequivalent nuclei—fluorines at the CF_3, α-CF_2, and β-CF_2 unit—giving rise to three resonances in the ^{19}F spectrum. In supercritical CO_2 each unit's behavior as a function of solvent density is quite different. At all temperatures, with increasing CO_2 density each unit responds with increased sensitivity from the center CF_2 unit (the β-CF_2) toward the end of the fluorinated chain (the CF_3 unit). The CF_3 units always experience a downfield shift of $\leq +0.4$ ppm. For the α-CH_2 unit, down- and upfield shifts can be monitored in the same experiment (i.e., at constant temperature) spanning a variance of about 0.1 ppm. On the other hand, the resonances of the inner β-CF_2 units are always shifted to higher field by ≤ -1.5 ppm. Similar effects were reported for $C(CH_2CH_3)_4$, $Si(CH_2CH_3)_4$, and $Sn(CH_2CH_3)_4$, where $\sigma_w(CH_3)$ was always found to be larger than $\sigma_w(CH_2)$. These latter results were interpreted in terms of the different accessibility of the individual sites. Correspondingly, solute and solvent−solute site factors have been introduced in the theoretical models no longer treating the solute and solvent as a point but rather as a spatially extended molecule.[26,41]

(4) Finally, in contrast to the proton chemical shifts of *n*-hexane which were basically independent of temperature, the perfluorinated analogue shows a distinct temperature effect for the ^{19}F chemical shifts. This effect can best be seen from the plot in Figure 3, where, as an example, the chemical shifts of the α-CF_2-unit are shown for the three different temperatures on the same scale as the proton data in Figure 1.

A higher temperature always results in a lower magnetic shielding. However, the effect is stronger for the α- and β-CF_2 units than for the terminal CF_3 group. The temperature effect has been studied in more detail in NMR experiments at constant CO_2 density (Figure 4). A density of 0.68 g cm^{-3} was chosen, and the temperature was increased from 27.2 to 73.9 °C.

A strictly linear relationship between the ^{19}F chemical shift and the temperature can be observed for all three sites in *n*-C_6F_{14}. While the proportionality factor for the temperature dependence is always positive—the resonances are always shifted downfield—the shift of the two CF_2 units is about twice as large as that for the CF_3 unit. Again, since the density was kept constant, there should be no contribution from the bulk susceptibility to these observations. Hence, we attribute this effect entirely to the temperature dependence of the intermolecular van der Waals interactions.

In summary, we conclude from our ^1H and ^{19}F NMR experiments that these nuclei behave dramatically differently in supercritical carbon dioxide. While for the protons the bulk susceptibility of the CO_2 is the only relevant factor, the fluorine nuclei experience an additional contribution attributed to magnetic shielding originating from van der Waals interactions. For pure fluorinated substances in the gas or liquid phase, such findings and interpretations are not new.[42] Therein, however, the interactions are between identical fluorinated molecules (A−A interactions). It should be emphasized that here we report evidence for van der Waals interactions between a fluorinated solute at low concentrations and carbon dioxide solvent (A−B interactions) where A−A contacts are negligible. In the next section we compare these results with similar measurements on 1,1-dihydroperfluorooctylpropionate (FOP), which corresponds to a monomeric unit of the CO_2-soluble macromolecule poly(1,1-dihydroperfluorooctylacrylate) (PFOA).

^1H and ^{19}F NMR Spectroscopy of 1,1-Dihydroperfluorooctylpropionate in Supercritical CO_2. In contrast to the two hexanes, FOP (see Figure 6 for the chemical structure) was used as a model for the CO_2-soluble polymer poly(1,1-dihydroperfluorooctylacrylate) (PFOA). PFOA is composed of a polyacrylate backbone with fluorinated side chains ($-CH_2-C_7F_{15}$) attached to the ester group; it may exhibit a strong dipole moment (about 3−4 D depending on conformation[43]). However, the presence of polar C−F bonds in the same molecule does not affect the behavior of the proton chemical shifts in supercritical CO_2 (Figure 5).

Although a slight temperature dependence is visible, the FOP proton chemical shifts show the same linear behavior as a function of the CO_2 density as found in *n*-hexane (see Figure 1). Again, the slopes (-1.8×10^{-6} cm^3 g^{-1} at 41.2 °C and

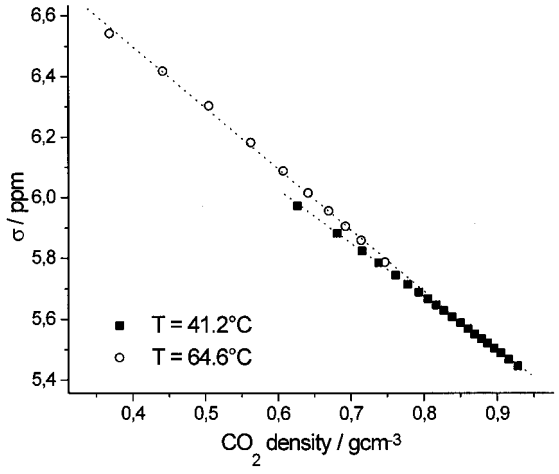

Figure 5. ^{1}H chemical shift of FOP ($-O-CH_2$ resonance) in CO_2 as a function of CO_2 density at $T = 41.2$ °C (○) and $T = 64.6$ °C (■). The $-CH_2$ and $-CH$ resonances showed the same behavior but are not displayed for clarity. All chemical shifts are given with respect to $CDCl_3$.

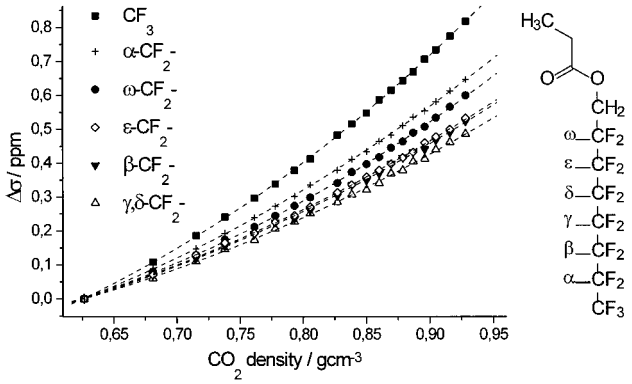

Figure 6. "Excess" shift, $\Delta\sigma = \sigma - \sigma_b - \sigma_{init}$, of the ^{19}F resonances of FOP in supercritical CO_2 at $T = 41.2$ °C with changing CO_2 density. The peak assignments are based on a $^{19}F-^{19}F$ COSY experiment.[36]

-2.0×10^{-6} cm^3 g^{-1} at 64.6 °C) match the anticipated influence of the CO_2 bulk susceptibility. (The splittings of the $-O-CH_2$ triplet as well as the CH_3 triplet and the $-CH_2$ quartet remain constant over the entire density region. The measured coupling constants of 13.6 and 7.6 Hz are in good agreement with the literature [$^3J(^1H-^{19}F) = 13$ Hz; $^3J(^1H-^1H) = 7-8$ Hz[44]] and indicate no change in the motionally averaged conformation of the FOP molecule in CO_2.) The proton data are consistent with an absence of specific solute−solvent interactions between CO_2 and hydrogenated sites in FOP.

On the other hand, looking at the fluorine chemical shifts of FOP in CO_2 gives almost identical results as those of perfluoro-*n*-hexane (Figure 6). ^{19}F NMR spectra were recorded at CO_2 densities between 0.37 and 0.93 g cm^{-3}; Figure 6 shows those "excess" changes in the shielding that are present after the influence of σ_b is removed ($T = 41.2$ °C).

There is no linear susceptibility-dominated relationship between the chemical shift and the CO_2 density, and second-order polynomials have to be used to fit the data. All of the four points discussed above for perfluoro-*n*-hexane—the presence of a contribution in addition to σ_b, the nonlinearity of the density dependence, the site specificity, and the temperature dependence—apply to the interpretation of the fluorine chemical shifts of FOP. In particular, the site-specific shifts along the fluorinated chain is apparent in the shielding with increasing CO_2 density. While the effect is the strongest for the CF_3 and the α-CF_2 unit (i.e., the units at the end of the chain exhibit an additional shift of about +0.8 and +0.65 ppm, respectively), it becomes weaker for the $-CF_2$ units in the middle of the fluorinated chain (β, γ, δ units), and finally, the effect emerges stronger again for the $-CF_2$ units close to the ester linkage (ϵ, ω units).

Site-Specific Shifts in C_6F_{14} and FOP. The similarity between the trends in the chemical shifts of the last three units in the fluorinated FOP chain and the three different units in perfluoro-*n*-hexane can be seen from the comparison of data in Figure 7a.

Therefore, we conclude that the same van der Waals interactions apply to both solvent−solute pairs, CO_2−FOP and CO_2−perfluoro-*n*-hexane. Despite the lack of a theory to explain these observed site-specific effects quantitatively, we applied the model suggested by Rummens et al.[26,27] and calculated the conformationally averaged surface area per fluorine atom for each of the three units in perfluoro-*n*-hexane.[45] The calculated values are 13 (CF_3), 11.8 (α-CF_2), and 10.3 Å^2 (β-CF_2). Normalizing the excess shielding effect discussed above by these calculated areas effectively collapses the density

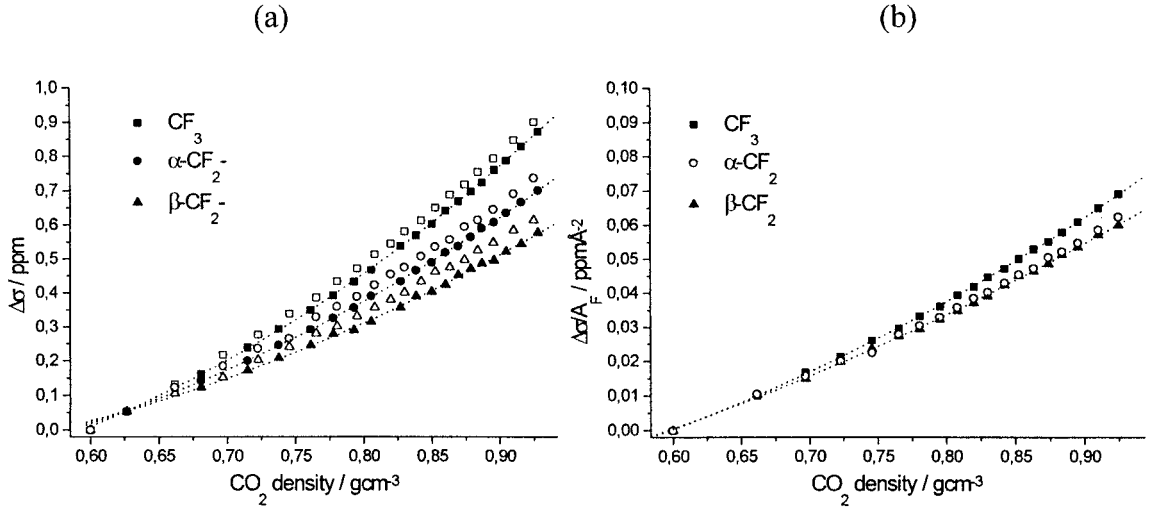

Figure 7. (a) Comparison of the changes in the excess shielding effect for perfluoro-*n*-hexane (open symbols) and FOP (solid symbols) with increasing CO_2 density. (b) Excess shielding $\Delta\sigma$ per fluorine surface area in perfluoro-*n*-hexane in CO_2. Note that the vertical scale is expanded by an order of magnitude.

dependence of the chemical shift for the different sites to a single curve (Figure 7b).

Although this simple model can be used to explain the different behavior at the three sites in the symmetric perfluoro-*n*-hexane molecule, for FOP there may be additional effects the closer the $-CF_2$ unit is to the ester linkage. Whether or not the carbonyl oxygen in the ester group itself has any specific interaction with CO_2 cannot be determined here. However, it was suggested by Kazarian et al.[46] that specific interactions between CO_2 and carbonyl groups in various polymers are the reason for altered C−O bending vibrations in the carbon dioxide, and furthermore, these interactions are believed to facilitate the swelling of these polymers in CO_2.

Conclusions

High-pressure, high-resolution NMR spectroscopy has been shown to be a powerful tool for studying solvent effects and solute−solvent interactions in supercritical and liquid CO_2. Excess chemical shift effects have been found in ^{19}F NMR of fluorinated solutes dissolved in CO_2 in contrast to the normal bulk susceptibility-dominated ^1H NMR observations in hydrocarbon solutes. In analogy to the gas- and liquid-phase NMR studies on pure fluorinated substances,[42] we attribute this excess magnetic shielding to van der Waals interactions between the fluorinated sites in the solute and carbon dioxide. The experiments reported here constitute the first spectroscopic evidence for specific intermolecular interactions in CO_2 involving fluorinated solutes. Our findings qualitatively corroborate the calculations of Cece[18] although the methods employed in those claculations have been criticized.[47] The identification of van der Waals interactions between fluorinated solutes and CO_2 which can be varied by changing CO_2 pressure and density represents a first step toward understanding the (tunable) solvent strength of CO_2 and may give new insights into polymer solubility in supercritical carbon dioxide.

Acknowledgment. This research is supported through a research fellowship from the Deutsche Forschungsgemeinschaft (A.D.) and a grant from the Consortium for Polymeric Materials and Processing in Carbon Dioxide at the University of North Carolina at Chapel Hill, sponsored by Air Products and Chemicals, Bayer, B.F. Goodrich, DuPont, Eastman Chemicals, General Electric, Hoechst-Celanese, and Xerox. A.D. thanks Dr. C. D. Poon for many discussions and his help running the spectrometer.

References and Notes

(1) Stofesky, D.; Reid, M.; Enick, R. M. In *Proceedings of the 2nd International Symposium on Supercritical Fluids;* McHugh, M. A., Ed.; Johns Hopkins University: Baltimore, MD, 1991.

(2) Johnston, K. P.; Penninger, J. M. L. *Supercritical Fluid Science and Technology*; *ACS Symp. Ser.* **1989**, *406*.

(3) Eckert, C. A.; Knutson, B. L.; Debenedetti, P. G. *Nature* **1996**, *383*, 313.

(4) McHugh, M. A.; Krukonis, V. J. *Supercrtitcal Fluid Extraction-Principles and Practice*; Butterworth-Heinemann: Boston, 1994.

(5) Hyatt, J. A. *J. Org. Chem.* **1984**, *49*, 5097.

(6) Consani, K. A.; Smith, R. D. *J. Supercrit. Fluids* **1990**, *3*, 51.

(7) Laintz, K. E.; Yonker, C. R.; Smith, R. D.; Wai, C. M. *J. Supercrit. Fluids* **1991**, *4*, 194.

(8) Wang, W. V.; Kramer, E. J.; Sachse, W. J. *J. Polym. Sci., Polym. Phys. Ed.* **1982**, *20*, 1371.

(9) Smith, P. B.; Moll, D. J. *Macromolecules* **1990**, *23*, 3250.

(10) DeSimone, J. M.; Guan, Z.; Elsbernd, C. S. *Science* **1992**, *257*, 954.

(11) DeSimone, J. M.; Maury, E. E.; Menceloglu, Y. Z.; Combes, J. R.; McClain, J. B.; Romack, T. J. *Science* **1994**, *265*, 356.

(12) McClain, J. B.; Betts, D. E.; Canelas, D. A.; Samulski, E. T.; DeSimone, J. M.; Londono, J. D.; Cochran, H. D.; Wignall, G. D.; Chillura-Martino, D.; Triolo, R. *Science* **1996**, *274*, 2049.

(13) Canelas, D. A.; Betts, D. E.; DeSimone, J. M. *Macromolecules* **1996**, *29*, 2818.

(14) Politzer, P.; Murray, J. S.; Lane, P.; Brink, T. *J. Chem. Phys.* **1993**, *97*, 729.

(15) Famini, G. R.; Wilson, L. Y. *J. Phys. Org. Chem.* **1993**, *6*, 539.

(16) Meredith, J. C.; Johnston, K. P.; Seminario, J. M.; Kazarian, S. G.; Eckert, C. A. *J. Phys. Chem.* **1996**, *100*, 10837.

(17) Yee, G. G.; Fulton, J. L.; Smith, R. D. *J. Chem. Phys.* **1992**, *96*, 6172.

(18) Cece, A.; Jureller, S. H.; Kerschner, J. L.; Moschner, K. F. *J. Phys. Chem.* **1996**, *100*, 7435.

(19) Johnston, K. P.; Penninger, J. M. L. *Supercritical Fluid Science and Technology*; *ACS Symp. Ser.* **1989**, *406*.

(20) Bright, F. V.; McNally, M. E. P. *Supercritical Fluid Technology: Theoretical and Applied Approaches in Analytical Chemistry*; *ACS Symp. Ser.* **1992**, *488*.

(21) Dickinson, W. C. *Phys. Rev.* **1951**, *81*, 717.

(22) Rummens, F. H. A. van der Waals Forces and Shielding Effects. In *NMR, Basic Principles and Progress*; Diehl, P., Fluck, H., Kosfeld, R., Seelig, J., Eds.; Springer-Verlag: Berlin, 1975; Vol. 10.

(23) Lau, E. Y.; Gerig, J. T. *J. Am. Chem. Soc.* **1996**, *118*, 1194.

(24) Bothner-By, A. A.; Glick, R. E. *J. Am. Chem. Soc.* **1956**, *78*, 1071; *J. Chem. Phys.* **1957**, *26*, 1647; *J. Chem. Phys.* **1957**, *26*, 1651.

(25) Bothner-By, A. A. *J. Mol. Spectrosc.* **1960**, *5*, 52.

(26) Rummens, F. H. A.; Bernstein, H. J. *J. Chem. Phys.* **1965**, *43*, 2971.

(27) Rummens, F. H. A.; Raynes, W. T.; Bernstein, H. J. *Chem. Phys.* **1968**, *72*, 2111.

(28) Bernstein, H. J.; Raynes, W. T. Presented at a NMR Symposium, Boulder, CO, 1962.

(29) Kromhout, R. A.; Linder, B. *J. Magn. Reson.* **1969**, *1*, 450.

(30) March, J. *Advanced Organic Chemistry*; John Wiley & Sons: New York, 1992; p 771.

(31) Pfund, D. M.; Zemanian, T. S.; Linehan, J. C.; Fulton, J. L.; Yonker, C. R. *J. Phys. Chem.* **1994**, *98*, 11846.

(32) Yonker, C. R.; Zemanian, T. S.; Wallen, S. L.; Linehan, J. C.; Franz, J. A. *J. Magn. Reson., Ser. A* **1995**, *113*, 102.

(33) Ely, J. F. *CO_2PAC: A Computer Program to Calculate Physical Properties of Pure CO_2;* National Bureau of Standards: Boulder, CO, 1986.

(34) *Handbook of Chemistry and Physics*; Chemical Rubber Company: Cleveland, OH, 1968.

(35) Pople, J. A.; Schneider, W. G.; Bernstein, H. J. *High-Resolution Nuclear Magnetic Resonance*; McGraw-Hill: New York, 1959.

(36) Dardin, A.; Samulski, E. T. Unpublished data.

(37) Buckingham, A. D.; Pople, J. A. *Discuss. Faraday Soc.* **1956**, *22*, 17.

(38) Raynes, W. T.; Buckingham, A. D.; Bernstein, H. J. *J. Chem. Phys.* **1962**, *36*, 3481.

(39) Kanegsberg, E.; Pass, B.; Carr, H. Y. *Phys. Rev. Lett.* **1969**, *23*, 572.

(40) Jameson, A. K.; Jameson, C. I.; Gutowsky, H. S. *J. Chem. Phys.* **1970**, *53*, 2310.

(41) Raynes, W. T. *Mol. Phys.* **1969**, *17*, 169.

(42) Jameson, C. J.; Jameson, A. K. *J. Phys. Chem.* **1980**, *73*, 6013. Jameson, C. J.; Jameson, A. K.; Oppusunggu, D. *J. Chem. Phys.* **1984**, *81*, 85, 1198, 2313, 2571. Jameson, C. J.; Jameson, A. K. *J. Magn. Reson.* **1985**, *62*, 209. Jameson, C. J. *Chem. Rev. (Washington, D.C.)* **1991**, *91*, 1375.

(43) Dipole moments were estimated from molecular simulation.

(44) Hesse, M.; Meier, H.; Zeeh, B. *Spectroscopic Methods in Organic Chemistry*; Georg Thieme Verlag: Stuttgart, 1987.

(45) Surface areas of CF_3, α-CF_2, and β-CF_2 were calculated for each possible conformation of the molecule using SIBYL with a MOPAC package and weighted with the Boltzmann factor.

(46) Kazarian, S. G.; Vincent, M. F.; Bright, F. V.; Liotta, C. L.; Eckert, C. A. *J. Am. Chem. Soc.* **1996**, *118*, 1729.

(47) Han, Y.-K.; Jeong, H. Y. *J. Phys. Chem. A* **1997**, *101*, 5004.